DOI 10.1007/s11182-020-02091-7
Russian Physics Journal, Vol. 63, No. 5, September, 2020 (Russian Original No. 5, May, 2020)

DEVELOPMENT KINETICS OF THE PLASTIC WAVE FRONT AT THE METAL INTERFACE

S. A. Barannikova and Yu. V. Li UDC 669.539.381.296

The paper considers an inhomogeneous development of plastic strain at the Chernov–Lüders band front in the bimetal consisting of carbon and austenitic steel layers. It is found that in the low carbon steel basal layer, the distribution of localized deformation at the yield point represents two zones similar to the Chernov–Lüders band. In the austenitic steel coating layer, the distribution of localized deformation at the yield point represents two plastic wave fronts similar to the Portevin–Le Chatelier effect. The paper proposes a mechanism of nucleation of localized deformation bands in the frame of the model of the solid fracturing.

Keywords: plasticity, deformation, localization, bimetal, Lüders bands.

INTRODUCTION

On the scale of the specimen size, macroscopic inhomogeneity and instability of plastic strain manifests itself in the form of the mutual stress-strain dependence $\sigma(\varepsilon)$ and localized strain patterns [1]. According to works [2–4], localized plastic strain during tension of metal alloys is realized in the form of either the Chernov–Lüders bands (also known as slip bands) at the yield point or the Portevin–Le Chatelier (PLC) effect during a discontinuous plastic strain [5]. The development kinetics of the Chernov–Lüders and PLC band fronts indicates both the similarities and differences between these phenomena [4]. As the similarity is concerned, it should be noted that the slip and the PLC band fronts represent macroscopic localizations of plastic strain in the form of narrow moving zones, in which plastic strain concentrates. The kinetics of the band evolution is similar, *viz*. in both cases the nuclei of localized plastic strain occur on the specimen lateral side and then grow across the whole cross-section. Significant differences in these phenomena are observed at a stage of developed localized plastic strain caused by the slip bands and the PLC effect [4]. Further investigations of these phenomena include the combined behavior of both slip and PLC band fronts during the tension of bimetal consisting of the carbon and austenitic stainless steels. Known models of strength physics and fracture mechanics used to describe the deformation and fracture of the solid material and individual components of laminated materials [6], do not allow estimating plastic strain localization and fracture at the layer interface. The purpose of this work is to analyze the macroscopic localized plastic strain under uniaxial tension of this bimetal [7].

LOCALIZED PLASTIC STRAIN OF BIMETAL AT THE YIELD POINT

The laminated metal consisting of carbon steel with the BCC crystal system and the austenitic stainless steel with the FCC crystal system were used in this experiment in the as-delivered condition [7]. The ASTM A414 grade A (st3sp) low carbon steel was used as a basal layer ~6.7 mm thick. The thickness of the top and bottom coating layers of

Institute of Strength Physics and Materials Science of the Siberian Branch of the Russian Academy of Sciences, Tomsk, Russia, e-mail: bsa@ispms.tsc.ru; jul2207@mail.ru. Translated from Izvestiya Vysshikh Uchebnykh Zavedenii, Fizika, No. 5, pp. 19–24, May, 2020. Original article submitted February 12, 2020.

the austenitic streel AISI 304 (12Kh18N9T) was ~0.75 mm. The steel sheet was prepared by hot rolling, from a three-layer ingot obtained by the addition of a hot metal (ASTM A414 grade A steel) between two coating AISI 304 steel sheets placed in a mould. The rolling temperature ranged between 1200–1400°C. That steel sheet could be considered as the material model for the investigation of the strain nucleation and propagation to the interface between the BCC and FCC metals. The tensile strength of the dogbone-shaped steel specimens 42×8×2 mm in size was measured on an LFM-125 Testing Machine (Walter + Bai AG, Switzerland) at 300 K and $6.67 \cdot 10^{-5}$ s^{-1} strain rate.

The stress-strain curve $\sigma(\varepsilon)$ of the bimetal specimens included the regions of elastic and plastic strains and fracture. The bimetal plastic strain curve located between two curves of its components [7, 8]. Similar to the ASTM A414 grade A specimen, the stress-strain curves of the AISI 304 specimen had the peak and the yield point, both appeared prior to those in the ASTM A414 grade A specimen. The mechanical properties of the laminated material differed from that of the bimetal components. The yield point of the bimetal approached to the yield point of the ASTM A414 grade A specimen, whereas the yield point of the AISI 304 specimen was higher than in the ASTM A414 grade A, but two times lower than in the AISI 304 specimen.

The bimetal yield point can be calculated by the mixture rule for composites [9]:

$$\sigma_T^{(\text{calc})} = \sigma_T^{(2)}(1-\alpha) + \sigma_T^{(1)} \cdot \alpha \,, \tag{1}$$

where $\sigma_T^{(1)}$, $\sigma_T^{(2)}$ are the yield points of the first and second bimetal components, α is the amount of the first component in the cross-section. In this case, the volume fraction of the first component (austenitic steel) is 0.19 and calculated as the ratio between its cross-sectional area and the total cross-sectional area of the bimetal. The volume fraction of the second component (low carbon steel) is 0.81. The yield points of the first and second components are 247 and 262 MPa, respectively. The bimetal yield point derived from Eq. (1) equals 260 MPa, the difference with the experimental value being ~4%.

The analysis of the microhardness distribution near the layer interface between AISI 304 and ASTM A414 grade A steels before and after tensile deformation at the end of the yield point, shows that in both states it is much higher than the microhardness of the basal and coating layers outside the layer interface [8]. Such a behavior of the microhardness in the bimetal transition zone is caused by the chemical and structural heterogeneity in the interfacial layer [8].

The microstructure and elemental composition of the interfacial layer were discussed in detail in [8]. Beyond the yield point, microcracks about (5 ± 1) μm long were observed in the coating layer, and the α'-phase formed as a result of the γ-α' phase transformation [10]. The amount of martensite α'-phase in the AISI 304 coating layer after the AISI 304 + ASTM A414 grade A bimetal tensile deformation was detected by the X-ray diffraction (XRD) analysis on a DRON-3 diffractometer using the monochromatized Cu K_α radiation. The XRD analysis of the AISI 304 surface layer in the bimetal showed that in the initial state, it contains only austenite (γ-phase) with the lattice parameters of a = 3.5999 Å. In bimetal specimens subjected to tensile deformation, the γ-α' phase transformation occurred in the AISI 304 surface layer [10] and the duplex structure was detected with different ratios of α'- and γ-phases. The total strain ε_{tot} = 15% provided ≈(52 ± 4)% of the martensite α'-phase (a = 2.8873 Å), the rest belonged to the austenite γ-phase. According to [6, 10], in the deformation-induced instable structure of the AISI 304 austenite steel, phase transformation might occur with the formation of α'-phase particles under the loading conditions. The PLC effect in varying the test temperature and the rate of tensile strain of metastable austenitic steel was studied in detail in [10].

It is stated that deformation of the bimetal components differs from plastic deformation of the three-layer steel consisting of the AISI 304, ASTM A414 grade A and AISI 304 layers. After tensile deformation of the bimetal comprising the layers with different mechanical properties, the additional internal stresses occur. Therefore, unlike the AISI 304 steel, in which the strain-induced γ-α' phase transformation occurs at high rates [10], the martensite transformation in the bimetal occurs in the AISI 304 thin coating layer soon afterwards the yield point. These structural changes affect the distribution of localized plastic strain during tension.

Let us consider the nucleation process of the slip bands in the bimetal at the yield point in real time, using the digital image correlation and tracking of speckle pattern on the surface [4, 7]. In the ASTM A414 grade A basal layer, a single wave front of localized elongation ε_{xx} is detected at the total strain of 0.006 at the yield point, whereas in the

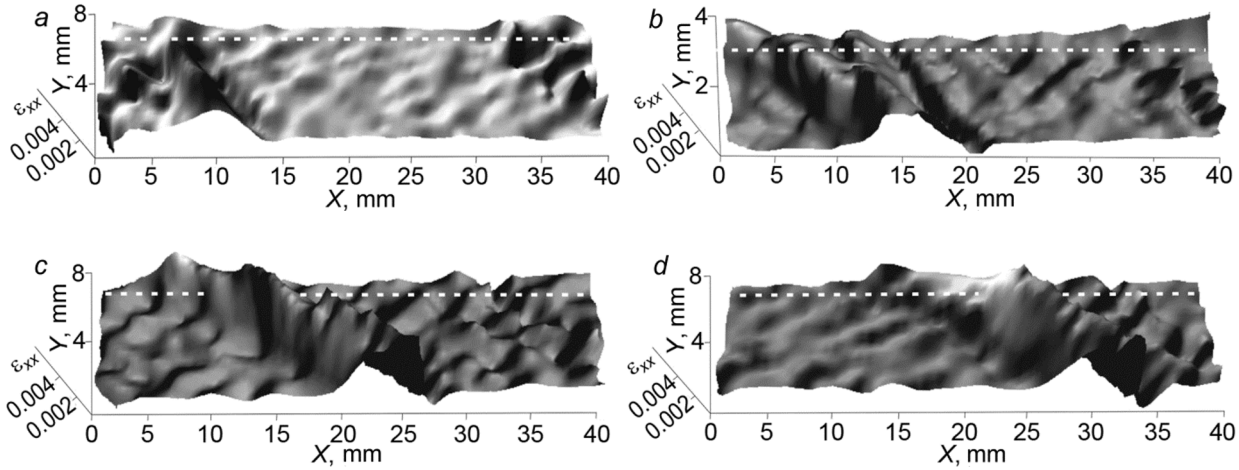

Fig. 1. Nucleation and propagation of Chernov–Lüders bands in the basal and coating layers of AISI 304 + ASTM A414 grade A + AISI 304 bimetal at different total strain: *a* – 0.006, *b* – 0.0074, *c* – 0.0081, *d* – 0.009. Dashed line indicates the layer interface.

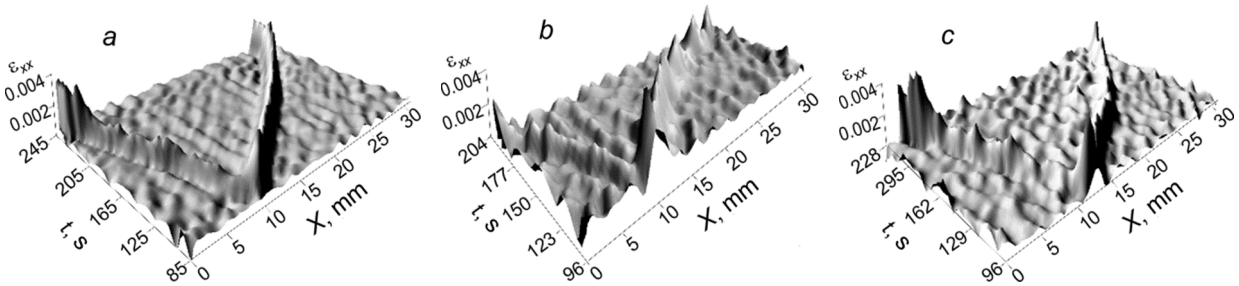

Fig. 2. Chernov–Lüders band propagation in AISI 304 + ASTM A414 grade A + AISI 304 bimetal at the yield point: *a* – ASTM A414 grade A basal layer, *b* – AISI 304 top coating layer, *c* – AISI 304 bottom coating layer.

AISI 304 coating layer, the localized elongation was not observed (Fig. 1*a*). This indicates that at the initial stage of plastic strain, macroscopic localized plastic strain nucleates in the form of the slip bands in the bimetal basal layer, which deforms prior to the coating layer. At a 0.007 total strain, the single maximum of localized elongations matching the localized plastic wave front, also occurs in the AISI 304 thin coating layer, when the slip band nucleus of the basal layer grows over the specimen width and reaches the layer interface. At this time, the slip band front of the basal and coating layers moves in the direction of the testing-machine head (Fig. 1*b–d*).

Thus, the analysis of the distribution patterns of the localized strain shows that at the early stages of plastic strain of the AISI 304 + ASTM A414 grade A + AISI 304 bimetal, the single slip band front occurs initially in the ASTM A414 grade A basal layer at the layer interface, and then initiates the nucleation of the slip band front in the AISI 304 coating layer. As shown in Fig. 2, the single wave front of localized elongation propagates throughout the yield point both in the basal and coating layers, whose material is not characterized by the slip bands at the initial stages of plastic strain.

For the solid AISI 304 steel specimen, the localized plastic wave fronts similar to that of the PLC effect, are observed at higher deformations at the stage of discontinuous plastic strain and caused by the interaction of carbon interstitial atoms with mobile dislocations in the martensite α'-phase resulting from the strain-induced γ-α' phase

transformation [10]. The slip bands in the coating layer may be produced due to the formation of martensite α'-phase, which is detected in the bimetal surface layer beyond the yield point.

It was found that the values of the local elongation ε_{xx} matching the slip bands in the basal (ASTM A414 grade A) and the coating (AISI 304) layers at the yield point, significantly differed in the local strain. A comparison was carried out using the Student's *t*-test. It turned out that the difference between the local elongation ε_{xx} of the basal and coating layers was significant, because the Student's *t*-test showed $|t| = 7.5 > 2.11$, *i.e.* $|t| > t_{\alpha,f}$, where the reference value of the Student's coefficient was $t_{\alpha,f} = 2.11$ at an $\alpha = 0.95$ confidence level. We then confirmed that at the yield point, both in the ASTM A414 grade A basal layer and the AISI 304 coating layer, two different bands of localized plastic strain were observed in each material, that were similar to the slip and PLC bands.

One of the most important parameters for the plastic strain localization is its front propagation velocity. As can be seen from Fig. 2*a*, at the bimetal yield point, two slip band fronts nucleating in the ASTM A414 grade A basal layer, move in opposite directions at different velocities of $V_1 = -1.5 \cdot 10^{-4}$ m/s and $V_2 = 1.2 \cdot 10^{-4}$ m/s, respectively.

During tension of the bimetal consisting of metals with different mechanical properties, plastic strain occurs initially in the layer of the soft metal, while the stronger coating loayer still undergoes elastic strain. Then, at the yield point, the basal and the coating layers are exposed to plastic strain. As shown in Fig. 2*b*, in the AISI 304 top coating layer, two plastic wave fronts of the PLC effect propagate in opposite directions at $V_1 = -0.7 \cdot 10^{-4}$ m/s and $V_2 = 2.3 \cdot 10^{-4}$ m/s, respectively. And in the AISI 304 bottom coating layer, two plastic wave fronts also propagate in opposite directions at $V_1 = -0.7 \cdot 10^{-4}$ m/s and $V_2 = 2.2 \cdot 10^{-4}$ m/s, respectively.

A comparison of the average front propagation velocity of localized strain in the bimetal layers with that of the solid specimens of the low carbon and austenitic stainless steel shows that at the yield point, $V_{av} = 1.35 \cdot 10^{-4}$ m/s in the basal layer of the low carbon steel, while in the solid specimen of the low carbon steel, it is $V_{av} = 0.85 \cdot 10^{-4}$ m/s. At the yield point in the coating layer of the austenitic steel the average front propagation velocity is $1.4 \cdot 10^{-4}$ m/s, and in the solid specimen of the austenitic steel, it is $0.15 \cdot 10^{-4}$ m/s during the linear strain hardening. Thus, during tension of the AISI 304 + ASTM A414 grade A + AISI 304 bimetal, the coating layer 750 μm thick does not prevent the formation of the Chernov–Lüders bands and increases their front propagation velocity in the basal layer of the low carbon steel and in the coating layer of the austenitic stainless steel in comparison with the individual components of the ASTM A414 grade A and AISI 304 steels.

RESULTS AND DISCUSSIONS

According to Fig. 1, in the AISI 304 + ASTM A414 grade A + AISI 304 bimetal, the single wave front of the slip band first occurs at the layer interface, in the ASTM A414 grade A basal layer. Then, it grows across the specimen width and reaches the opposite layer interface, which is typical for low carbon steels at the yield point. In austenitic steels, the formation of the single wave fronts of localized strain at early stages has not been not previously observed.

To understand the PLC effect in the AISI 304 coating layer, let us use the fracturing model proposed by Barenblatt [11]. Fracturing is the crack formation in a solid due to entering a rigid wedge into it. During the metal delamination, the bonding strength acting between the opposite sides of the solid are overcome gradually, and the crack edges close, thereby forming a smooth profile, as is the case for separating two glued pieces from each other [11]. A smooth closure of the crack edges and the stress finiteness is a condition to determine the size of an equilibrium crack during the solid fracture [11]:

$$l = \frac{E^2 \cdot h^2}{4(1-\mu^2)^2 K^2}. \qquad (2)$$

Here E is the Young's modulus, h is the wedge width, μ is the Poisson ratio, K is the modulus of cohesion, which describes the bonding strength between the crack edges (material constant). On the one hand, the bonding strength is effective only in the small vicinity of the crack tip. On the other, in the area of the actual bonding strength, the surface

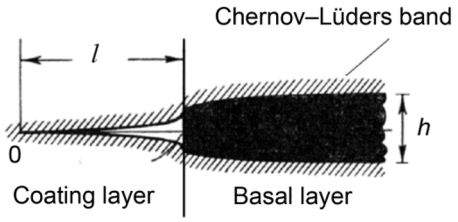

Fig. 3. Chernov–Lüders band as wedge element in the model of bimetal fracturing.

force density is several orders of magnitude higher than stresses in this place enabled by the external loads without cracking [11].

Figure 3 schematically illustrates the fracturing model, which is applied to the nucleation of the PLC effect in the coating layer at the yield point. And the slip band in the ASTM A414 grade A basal layer is considered as a wedge. Substituting $E = 2 \cdot 10^5$ MPa; $h = 10^{-4}$ m (the front width of the slip bands in the basal layer); $\mu = 0.3$ (Poisson ratio); and $K = 2.5 \cdot 10^3$ MPa·m$^{1/2}$ (the modulus of cohesion for carbon steel) [11] in Eq. (2), we obtain the length l of about 20 μm for the crack formed behind the wedge in the coating layer. As mentioned above, a microcrack ≈(5 ± 1) μm long is detected in the austenitic-steel coating layer. It can be argued, therefore, that the fracturing force created by the slip band front in the basal layer, forms a microcrack several micrometers long, which causes the elastic stress concentration in the coating layer.

The stress concentration at the slip band front in the ASTM A414 grade A basal layer nearby the metal interface can be calculated from

$$\sigma_{xx} = E\varepsilon_{xx}, \tag{3}$$

where $E = 2 \cdot 10^5$ MPa is the Young's modulus, ε_{xx} = 0.014 is the average localized elongation of the bimetal component. The stress concentration at the slip band front is then 2800 MPa.

The stress concentration σ_* at the crack tip in the coating layer and at the slip band front in the ASTM A414 grade A basal layer increases due to the contribution of the local stresses caused by the higher microhardness at the layer interface. They can be roughly estimated from [12]

$$\sigma_* = H_v(1 - \mu - 2\mu^2), \tag{4}$$

where $H_v = 3500$ MPa is the maximum microhardness at the AISI 304 layer at the yield point; $\mu = 0.3$ is the Poisson ratio. According to Eq. (4), the stress concentration caused by the chemical and structural heterogeneity in the bimetal interlayer, is 1750 MPa.

Thus, this work shows for the first time that the slip band nucleated at the yield point of the ASTM A414 grade A basal layer can play the role of a wedge in the Barenblatt fracturing model, thereby initiating the crack formation in the coating layer. Due to the high stress concentration at the layer interface, the latter promotes the formation of the martensite α'-phase during the strain process at the yield point. The nucleation mechanism of the PLC band fronts detected at a higher, discontinuous plastic strain of 700 MPa, activates in the AISI 304 coating layer.

In accordance with the force criterion of the fracture mechanics, Makhutov [13] proposed to evaluate the stress concentration σ_c in the microcrack nucleation region as

$$\sigma_c = \frac{K_{Ic}}{\sqrt{2\pi l}}, \quad (5)$$

where K_{Ic} is the critical stress intensity factor. According to the microanalysis and the reference value of $K_{Ic} = 25$ MPa·m$^{1/2}$ for the AISI 304 steel [13], the critical value of the stress concentration is 4460 MPa at ≈5 μm long crack in the AISI 304 coating layer near the layer interface, and approaches to the total stress concentration ($\sigma_\Sigma = \sigma_{xx} + \sigma_* = 4550$ MPa) at the interface calculated from Eqns (4) and (5). In other words, the condition of the crack propagation in the AISI 304 coating layer is satisfied, when the stresses reach the critical value, according to the force criterion of the fracture mechanics $K_I = K_{Ic}$ [13]. However, after the yield point, the bimetal does not fracture, because in the bimetal as well as in laminated composite materials [9], the layer interface prevents the crack development. Nevertheless, the defect accumulation in the coating layer occurs more intensively than in the basal layer. Since $K_{Ic} = 49$ MPa·m$^{1/2}$ [13] for the basal layer, at the interfacial microcrack ≈5 μm long, the critical stress concentration is 8750 MPa (see Eq. (5)), *i.e.* less, than for the austenitic steel. Therefore, the crack generated at the layer interface, begins to grow into the coating layer.

CONCLUSIONS

Based on the method of the digital image correlation and tracking of speckle pattern, the macroscopic localized plastic strain was investigated in the real time conditions, under the bimetal uniaxial tension, that allowed us to determine the localized strain distribution in different bimetal layers such as AISI 304, ASTM A414 grade A and AISI 304 steels.

It was found that the Chernov–Lüders band originated from the layer interface, in the ASTM A414 grade A basal layer provided the crack formation in the AISI 304 coating layer at stresses equaled the bimetal yield point. Owing to high stress concentration at the layer interface, the Chernov–Lüders band contributes to the formation of the martensite α'-phase at the yield point and the nucleation of the PLC band front in the AISI 304 coating layer. During tension of the solid AISI 304 steel specimens, the localized plastic wave fronts were observed at higher deformations at the stage of a discontinuous plastic strain.

It was also shown that during tension of the AISI 304 + ASTM A414 grade A + AISI 304 bimetal, the AISI 304 coating layer 750 μm thick did not prevent the formation of the Chernov–Lüders bands and provided the increase in the front propagation velocity of these bands both in the basal and coating layers when compared with the individual components of the ASTM A414 grade A and AISI 304 steels.

This work was carried out within the government contract N III.23.1.2 of the Institute of Strength Physics and Materials Science SB RAS.

REFERENCES

1. S. A. Barannikova, A. V. Ponomareva, L. B. Zuev, *et al*., Solid State Commun., **152**, No. 9, 784–787 (2012).
2. M. A. Lebyodkin, D. A. Zhemchuzhnikova, T. A. Lebedkina, *et al*., Results Phys., **12**, 867–869 (2019).
3. A. F. Shibkov, M. F. Gasanov, M. A. Zheltov, *et al*., Int. J. Plasticity, **86**, No. 1, 37–55 (2016).
4. L. B. Zuev, J. Appl. Mech. Tech. Ph., **58**, No. 2, 328–334 (2017).
5. J. Pelleg, Mechanical Properties of Materials, Springer, Dordrecht (2013).
6. E. S. Gorkunov, S. M. Zadvorkin, and E. A. Putilova, Russ. J. Nondestruct., **48**, No. 8, 495–504 (2012).
7. S. A. Barannikova, A. V. Bochkareva, Yu. V. Li, *et al*., Izv. Vyssh. Uchebn. Zaved., Fiz., **59**, No. 7/2, 8–12 (2016).
8. G. V. Shlyakhova, S. A. Barannikova, A. V. Bochkareva, *et al*., Steel Transl., **48**, No. 4, 219–223 (2018).

9. T. Fudzii and M. Dzako, Fracture Mechanics of Composite Materials [Russian translation], Mir, Moscow (1982).
10. A. Müller, C. Segel, M. Linderov, *et al*., Metall. Mater. Trans. A: Phys. Metall. Mater. Sci., **4,** No. 1, 59–74 (2016).
11. G. I. Barenblatt, J. Appl. Mech. Tech. Ph., **23**, No. 3, 622–636 (1959).
12. Yu. V. Milman, S. I. Chugunova, and I. V. Goncharova, Bulletin of the Russian Academy of Sciences: Physics, **73**, No. 9, 1215–1221 (2009).
13. N. A. Makhutov, Structural Strength, Operational Life and Technogenic Safety [in Russian], vol. 1, Nauka, Novosibirsk (2005).